LA-9612-MS

C.3

Oblique Interactions of Detonation Waves

with Explosive/Metal Interfaces

Los Alamos
Los Alamos National Laboratory
Los Alamos, New Mexico 87545

DISCLAIMER

Oblique Interactions of Detonation Waves with Explosive/Metal Interfaces

J. M. Walsh

Los Alamos National Laboratory
Los Alamos, New Mexico 87545
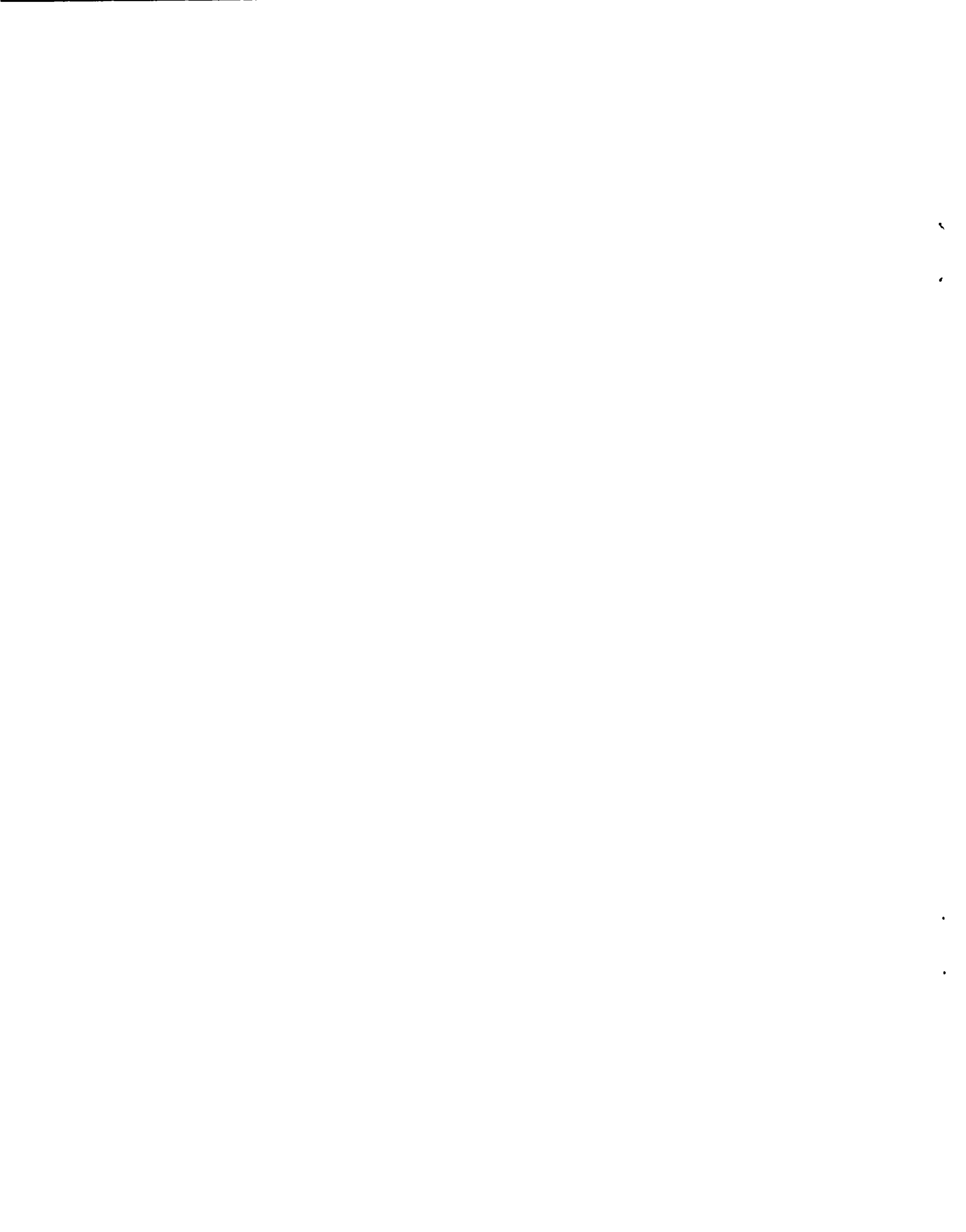
OBLIQUE INTERACTIONS OF DETONATION WAVES WITH EXPLOSIVE/METAL INTERFACES

by

J. M. Walsh

ABSTRACT

The interaction of a detonation wave with an explosive/metal interface is considered. Theoretical models are discussed, and calculated results are given for PBX 9501 onto uranium, tantalum, copper, 304 stainless steel, aluminum, and nickel.

For PBX 9501 onto aluminum and copper, regular shock reflection (in the PBX 9501) at small angles changes to regular rarefaction reflection (Prandtl-Meyer flow) at large angles, and the curve of metal-shock pressure vs incidence angle is smooth. For the other metals, there is a discontinuity in shock pressure where low-angle, regular reflection transits to Mach reflection, and a smaller discontinuity where the Mach reflection changes back to high-angle regular reflection.

I. INTRODUCTION AND SUMMARY

In most explosive/metal systems, a detonation wave impinges upon an explosive/metal interface. Such interactions are discussed, and numerical results are given in the main text for the case of PBX 9501 on uranium. Similar results for PBX 9501 onto tantalum, copper, 304 stainless steel, aluminum, and nickel are given in the Appendix.

Prior work has, of course, been very helpful. H. M. Sternberg and D. Piacesi[1] discuss such flows and give results for pentolite on iron. In their treatment of the Mach reflection regime, they make the basic simplifying assumption that the Mach stem does not grow. The associated assumption that the stem is appropriately curved then allows them to match the flow conditions at the triple point (top of stem) and at the explosive-metal interface (stem bottom). Later, M. T. Thieme* at Los Alamos National Laboratory used the Sternberg-Piacesi model to treat the interaction between PBX 9501 and uranium.

---

*M. T. Thieme, Los Alamos National Laboratory, provided this information (1979).

The closely related problem of shock-wave interactions within condensed explosives has also received considerable attention. S. D. Gardner and J. D. Wackerle[2] made flash-radiograph and sweep-camera measurements on several explosives and compared their results with theoretical models for regular and Mach reflection. They also gave a good summary of the related literature. Somewhat later, A. K. Oppenheim et al.[3] gave an extensive discussion of the possible wave interactions within explosives, both gaseous and condensed. Their discussion is aimed largely at understanding the microstructure of detonations.

In the model used in the present calculations, the Mach stem is allowed to grow, but it is taken to be straight. The resulting flow seems to be unobjectionable as a theoretical solution, but it should be pointed out that other valid solutions may exist in which the stem is curved. In fact, the most acceptable physical model of Mach flow may well involve a combination of stem growth and stem curvature, instead of invoking one or the other to meet boundary conditions. In that case, however, we see no way to determine the correct mix of the two mechanisms. Considerations outside the scope of the present ones (like considerations of the transient flow leading to the steady state that is assumed here, or considerations of heat conduction and viscosity within the flow) appear to be required.

A couple of quantitative comparisons were made using the Sternberg-Piacesi model and the present one. Agreement was very good for the cases examined, giving some support to the no-stem-growth approximation and/or the straight-stem assumption. Good general agreement is also obtained with the earlier calculations by Thieme,* despite the model difference and the small equation-of-state differences.

An interesting difference should, however, be noted. Sternberg and Piacesi,[1] and apparently Oppenheim et al.,[3] find that the reflected shock in the Mach regime is forward facing; that is, it is oriented such that it deflects the flow toward the interface in the steady-state coordinate system. Our calculated reflected shock is backward facing so that it deflects the flow away from the interface. As pointed out in the text, the difference is apparently caused by equations of state and not by flow-model differences.

Insofar as shock pressure P into the metal as a function of the incidence angle A is concerned, the principal results (for PBX 9501 onto uranium) are as follows:

---

*M. T. Thieme, Los Alamos National Laboratory, provided this information (1979).

(1) In the regular regime (A = 0° to A = 58.1°), shock pressure decreases from 610 kbar at head-on (A = 0°) incidence to 561 kbar at A = 53° and thereafter rises <u>sharply</u> (A = 53° to A = 58.1°) to 584 kbar at A = 58° and 609 kbar at the A = 58.1° breakdown of the regular reflection solution.

(2) The transition to Mach reflection at A = 58.1° is accompanied by a discontinuous jump in P to 640 kbar and a drop in P thereafter as A is increased.

(3) Between A = 77.7° and A = 79.3°, there is a 1.6° band where regular shock reflection again occurs. At 78°, for example, the shock pressure is 375 kbar compared with the Chapman-Jouguet pressure of 349 kbar.

(4) From A = 79.3° to A = 90°, a rarefaction is reflected into the HE, and the shock pressure in the uranium is less than the Chapman-Jouguet pressure.

II. EQUATION OF STATE

The metal equation of state is based upon a linear relationship between shock-wave velocity U_s and shock-particle velocity U_p,

$$U_s = C_o + SU_p \quad ,$$

and on the additional assumption that

$$\left(\frac{\partial P}{\partial E}\right)_V = \rho_o \gamma_o$$

is constant. Both approximations are widely used and give a satisfactory description of shock waves in the pressure range of interest here. (Constants C_o, S, ρ_o, and γ_o for the various metals are listed in Ref. 4. There, also, flow deflection by a stationary shock is discussed, and some of these results will be used below.)

For PBX 9501, an equation of state, also primarily a fit of experimental data, was provided by W. C. Davis** of Los Alamos National Laboratory. The isentrope through the Chapman-Jouguet point is taken to be

---

** W. C. Davis, Los Alamos National Laboratory, provided this information (1982).

$$P_i = P_{cj}\left(\frac{\rho}{\rho_{cj}}\right)^\gamma \quad ,$$

and states not on this isentrope are calculated by assuming that

$$\alpha = \frac{1}{V}\left(\partial E/\partial P\right)_V = 0.3$$

is a constant. The explosive initial density is $\rho_0 = 1.833$ g/cm^3; the detonation velocity is $D = 8.8 \times 10^5$ cm/s and $\gamma = 3.07$. Resulting values (using the Chapman-Jouguet condition) for the Chapman-Jouguet state are $P_{cj} = 3.4876 \times 10^{11}$ dyne/cm^2 and $\rho_{cj} = 2.430$ g/cm^3.

III. REGULAR REFLECTION REGIME AT SMALL ANGLES OF INCIDENCE

Regular reflection, sketched as Fig. 1, occurs when the angle of incidence A is small.

The well-known method of solution is also indicated in the figure. The P vs ϕ shock polars are calculated for the metal shock wave (see, for example, Ref. 4) and for the reflected shock wave into the explosive. The boundary conditions that the pressure P and the flow deflection ϕ must each be the same on the two sides of the interface then imply that the intersection of the two polars is the solution to the problem.

Actually, there are two solutions. The upper intersection of the polars (the strong root not pictured in the sketch) is discarded as physically unrealistic, partly because it indicates a very large jump in reflected shock pressure (above the well-known, head-on value) as A is increased from A = 0. We assume that the weak root is correct.

If A is increased (to about 58.1° for PBX 9501 onto uranium), we eventually reach a point at which the two polars no longer intersect, indicating that the regular reflection flow is no longer a solution to the problem. Beyond this critical A, there is a regime of Mach reflection. The Mach reflection flow is discussed next. (Later, a summary discussion is given showing the shock polars for the various reflection regimes.)
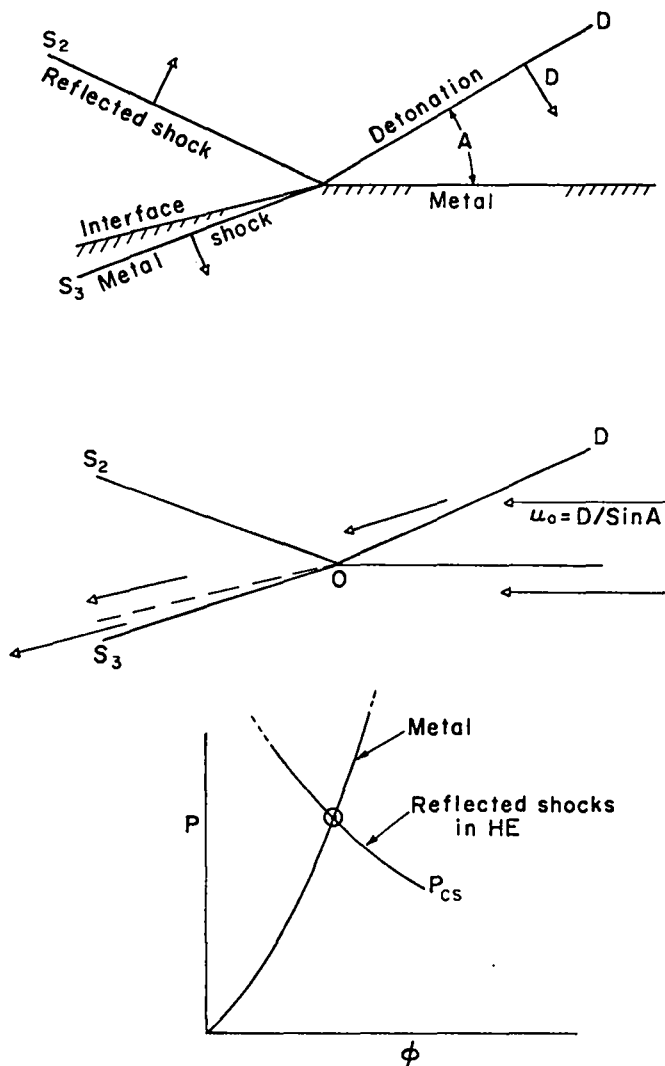
4

Fig. 1. Regular reflection.

IV. MACH REFLECTION AT INTERMEDIATE ANGLES OF INCIDENCE

Mach reflection (see Fig. 2) occurs because (for fixed angle A and detonation velocity D) the reflected shock S_2 can no longer straighten the flow.

In the Mach reflection flow, there are actually two distinct flows that can be reduced locally to steady-state flows by an appropriate choice of origins. If the origin is taken to be the moving point of intersection of the Mach stem and the metal interface ($\bar{0}$ in Fig. 2), the interaction of the Mach stem (a super Chapman-Jouguet detonation, calculable from the equation of state given in Sec. II) and the metal shock is a simple shock polar problem, the solution of which is indicated in the bottom left sketch of Fig. 2. This problem is solved in coordinate system $\bar{0}$ where the entry-flow velocity is $\bar{U}_o$.
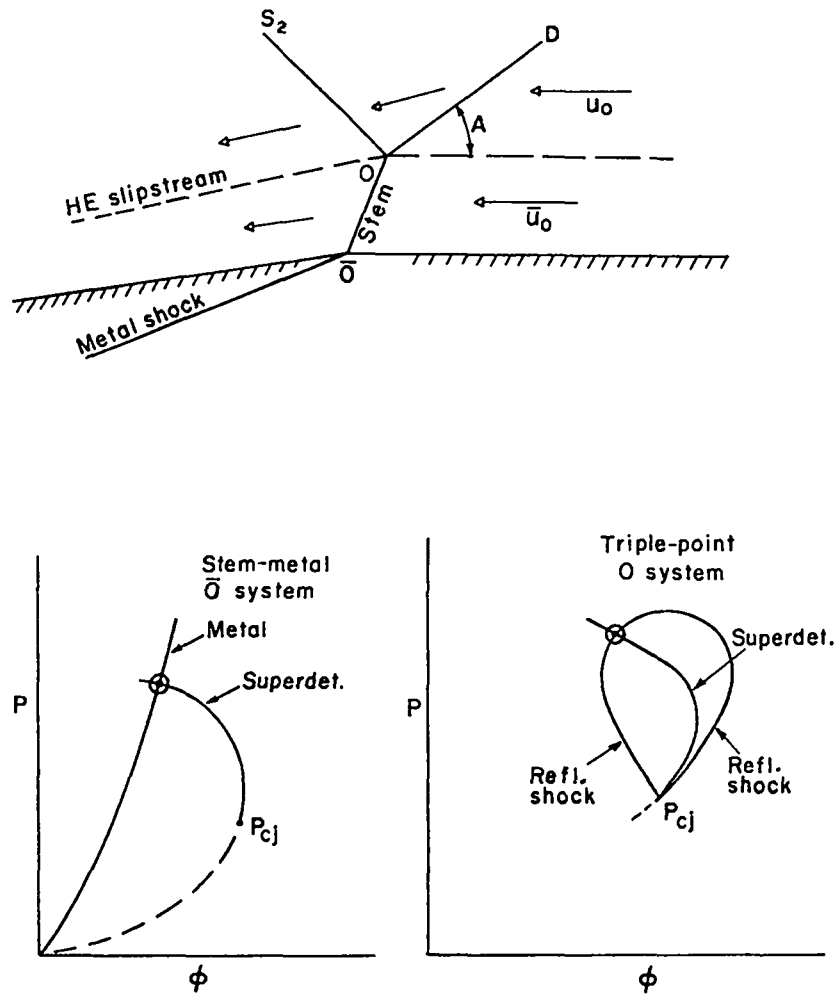
Fig. 2. Mach reflection. Here, $\bar{U}_0$ is entry-flow velocity relative to an origin at $\bar{0}$, and U_0 is entry-flow velocity relative to an origin at 0. A is the angle of the detonation front relative to the undisturbed interface.

The shock polar diagram for the triple-point problem is indicated at the bottom right of Fig. 2. The pear-shaped curve is the P vs ϕ locus for reflected shocks. The left half of this curve is for <u>backward-facing</u> shocks that decrease the flow deflection. The right half corresponds to forward-facing shocks. The super detonation curve, corresponding to the stem, is also shown in the sketch. The intersection of this curve and the reflected shock curve is the solution to the flow at the triple point. This problem must be solved in coordinate system 0, where the entry-flow velocity is U_0. The vector difference, $U_0 - \bar{U}_0$, is the rate of growth of the Mach stem.

Some remarks about the calculational details are in order. Because U_0 and $\bar{U}_0$ cannot be independently specified, an iteration procedure was necessary. In the procedure used, $\bar{U}_0$ was specified and the stem-metal problem was solved in the $\bar{0}$ system. This gives a complete description of the flow adjacent to the metal. In particular, the pressure P_s behind the stem (that is, the pressure in the whole region bordered by the metal shock, the stem, and shock S_2) and the inclination angle of the Mach stem are determined. (The velocity of the stem relative to the undetonated explosive is, of course, just $\bar{U}_0$.)

Next, the triple-point problem is solved in the 0 system for a _trial_ value of the angle A. Specifically, the trial A and known detonation velocity D give the velocity of the detonation front relative to the undetonated explosive. Then from the known stem velocity (above) and detonation velocity, it is simple to calculate the velocity of their intersection relative to the state ahead. The negative of this velocity is, therefore, the velocity U_0 at which the undetonated explosive enters the 0 system. (U_0 has a small negative component in the vertical direction, corresponding to positive stem growth.) Known boundary conditions are the required pressure P_s behind shock S_2 and the flow direction ϕ in that region. (To get ϕ, the velocity vector behind the stem in the $\bar{0}$-coordinate system is corrected over to the 0-coordinate system by using the known velocity vector difference, $U_0 - \bar{U}_0$, between the two systems.) To summarize, one has a required P_s behind S_2 and, for trial A, consequent values of U_0 and ϕ. To obtain a solution then, A is varied and the triple-point solution (bottom right of Fig. 2) is repeated until ϕ at P_s is correct.

Numerical results for one particular flow ($\bar{U}_0$ = 1.16, D = 1.0208 x 10^6 cm/s) are given as Fig. 3. For this example, A = 60.143° and P_s = 0.6076 Mbar. In the 0-coordinate system, the flow is deflected initially by 0.8743°, experiences an additional downward deflection of 7.5083° across the detonation front, and is deflected upward by about 2.618° by the S_2 shock. The resulting final deflection is 5.744°.

As already mentioned, the Mach reflection region (for PBX 9501 onto uranium) extends over some 20° from A = 58.1° to A = 77.7°. Actually, Mach reflection is a theoretically possible solution at both slightly smaller and slightly larger values of A, but we presume that the simpler regular reflection occurs when it is a possible flow. This overlap of the regular and Mach regimes will be discussed further below.
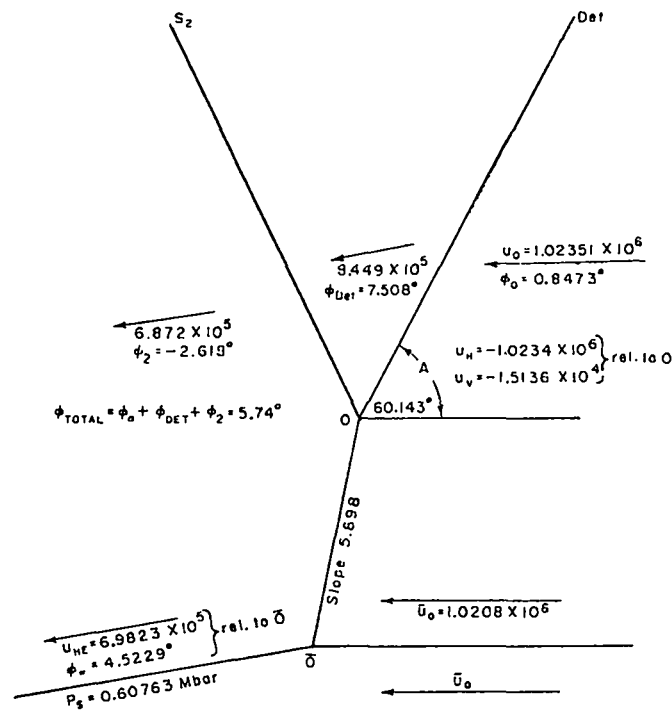
S_2

Det

$U_o = 1.02351 \times 10^6$

9.449×10^5
$\phi_{Det} = 7.508°$

$\phi_o = 0.8473°$

6.872×10^5
$\phi_2 = -2.619°$

$U_H = -1.0234 \times 10^6$
$U_v = -1.5136 \times 10^4$ rel. to O

$\phi_{TOTAL} = \phi_o + \phi_{DET} + \phi_2 = 5.74°$ O   60.143°   A

Slope 5.698

$\bar{U}_o = 1.0208 \times 10^6$

$U_{HE} = 6.9823 \times 10^5$ rel. to Õ
$\phi_s = 4.5229°$

Õ

$P_s = 0.60763$ Mbar

$\bar{U}_o$

Fig. 3.   Numerical results for a parti-
cular Mach reflection, PBX 9501
onto uranium. Note: The value
of ϕ_w (corrected to the coordi-
nate system at O) becomes 5.74°
in agreement with the upper flow.

As noted previously, our calculated reflected shocks are all backward facing
(or upward deflecting), as opposed to shocks calculated in prior studies (Refs. 1
and 3).

For a couple of flow configurations, we applied the Sternberg-Piacesi model
to our materials and obtained results in close agreement with the present (more
tedious) model. Their model is seen as Fig. 4. They assume that the stem does
not grow so that the whole process is steady state and can, therefore, be solved
in a single polar diagram. To meet the different boundary conditions at the
metal interface and at the triple point, they permit the stem to curve by the
necessary amount. The polar-diagram solution to this problem is given in the
bottom half of Fig. 4. This solution results in a slightly higher pressure P_1 at
the interface than the pressure P_2 at the triple point. Behind the Mach stem,
the flow must be converging in this model, but it is not necessary to treat that
part of the flow to obtain the cited results. Finally, the reflected shocks
remain backward facing, even though the Sternberg-Piacesi model is used. Hence,
the difference between their published results (pentolite explosive onto iron for
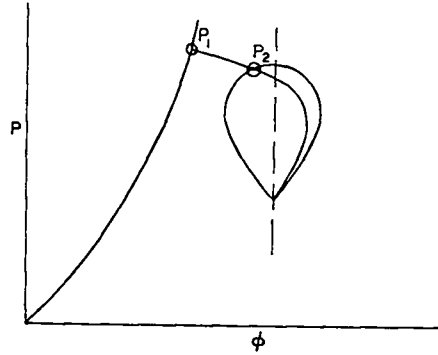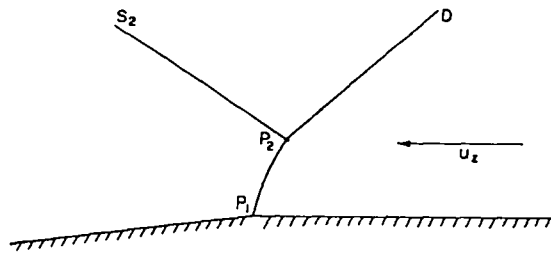
8

Fig. 4. Sternberg-Piacesi curved-
stem, steady-state model
for Mach reflection.

which they found forward-facing reflected shocks) and our present results is
apparently an equation-of-state difference rather than a difference resulting
from the different flow model.

Finally, it should be noted that the calculated reflected shock in Mach
reflection is a so-called strong root (the same deflection ϕ could have been
achieved with a weaker shock--see Fig. 2 or Fig. 4). This differs from regular
reflection where both roots are theoretically possible and the weak root is
assumed.

V.   SHOCK POLAR PLOTS AND THE VARIOUS REFLECTION REGIMES

Figure 5 is a series of nine shock polar plots for various values of the
angle A. In each case, the curve from the origin is the polar for the uranium.
Only the lower part of this polar is shown; the complete polar comes back to
$\phi = 0$ at a much higher P. The other curve in each plot is the polar for
reflected shocks into the Chapman-Jouguet state of the explosive. The Chapman-
Jouguet state is plotted as a triangle, and only the lower left lobe of each
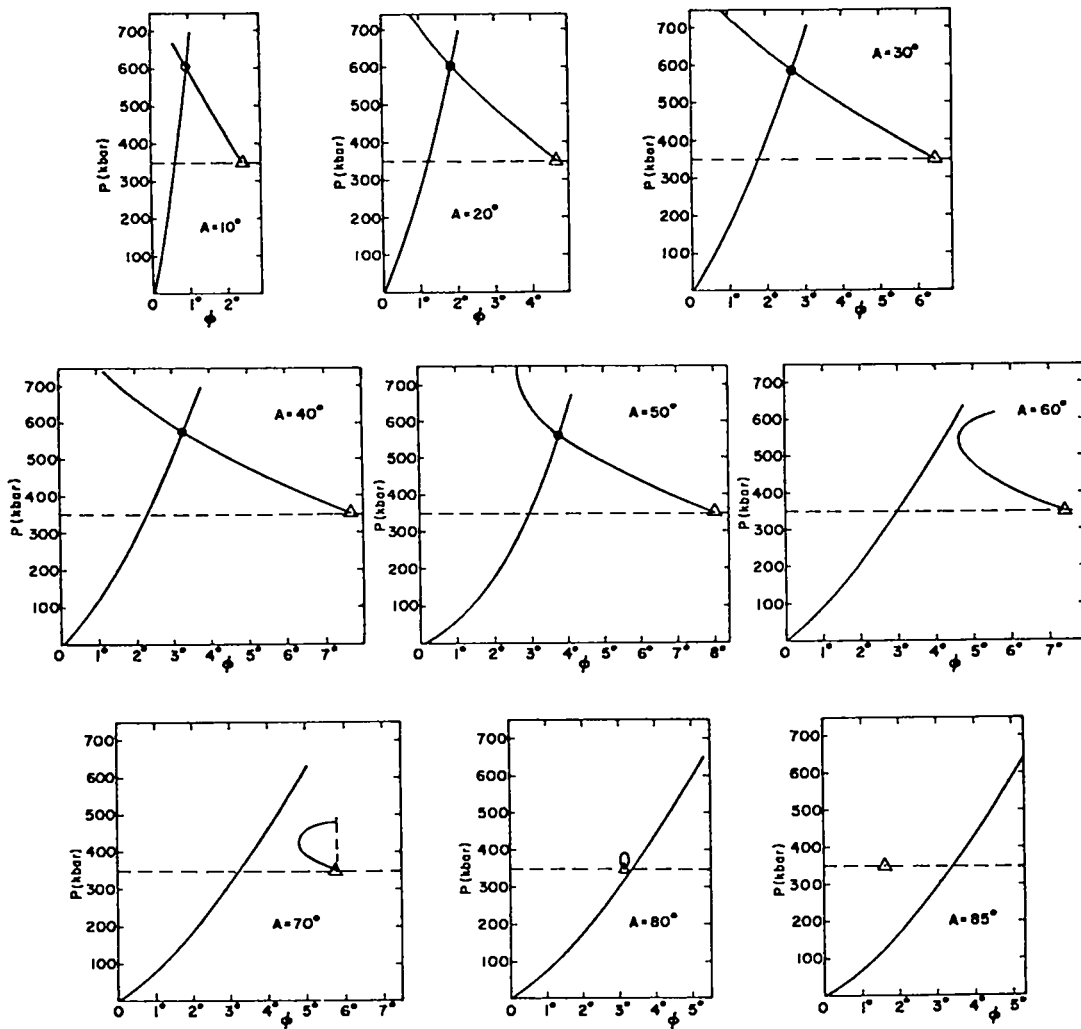
Fig. 5. Shock polars for various values of the interaction angle
A, explosive PBX 9501 onto uranium.

polar is shown for A ≤ 50°. For larger values of A, more of the polar is
included. The complete polar is always symmetrical about a vertical line through
the Chapman-Jouguet state.

It is seen that regular reflection solutions (plotted as circles) are possi-
ble for A ≤ 50° and not possible for A = 60°. This is compatible with an
observed tangency point at A = 58.1°. At larger A, the explosive polar is seen
to become smaller and to move leftward across the polar for the metal. The two
polars overlap between A = 77.7° and A = 79.3° so that regular reflection (with a
backward-facing reflected shock) is again possible in this narrow range. The
solution at A = 78°, for which the shock is backward facing, is seen as Fig. 6.
At A = 79.3°, this reflected shock has zero strength, and for 79.3° < A < 90°,
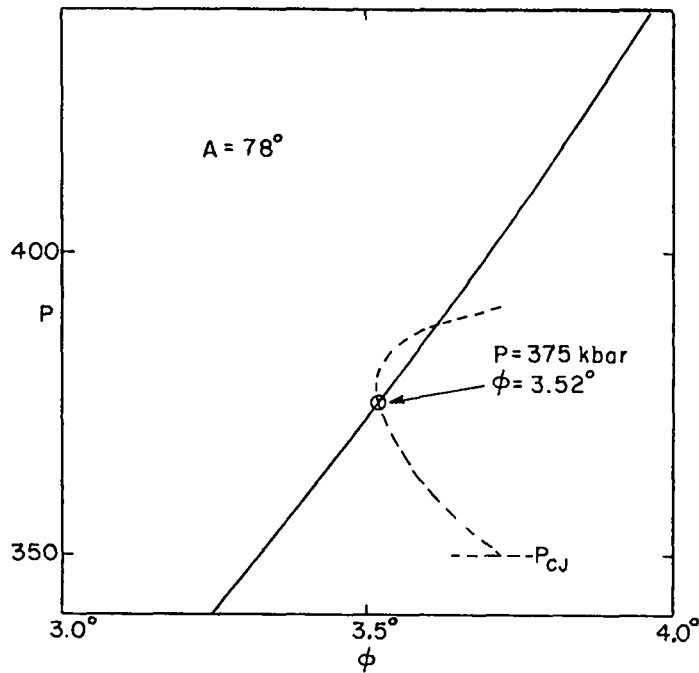the reflected wave is a rarefaction, as mentioned below.

10

Fig. 6. Regular reflection solution in the large A regular reflection regime.

Mach solutions are theoretically possible between A = 57.38° (some 0.7° before the breakdown of regular reflection) and A = 77.85° (some 0.15° after the onset of large A regular reflection). Within this range of theoretically possible Mach flows, the stem-growth rate is positive (being zero at the end points of the range). Mach "solutions" are also possible at larger and smaller A, but the associated stem-growth rates are negative, and these solutions are, therefore, rejected as nonphysical.

Figure 7 is a bar chart of the various reflection regimes, and Fig. 8 is a plot of metal shock pressure vs A. Between A = 79.3° (at which point the
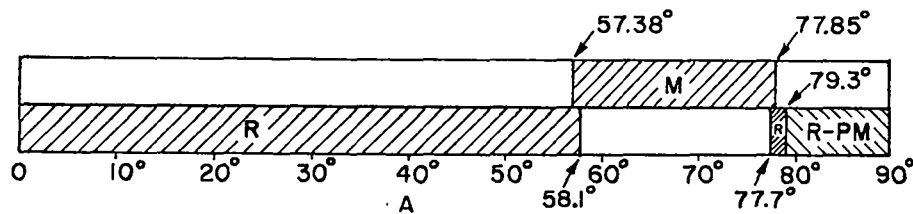

Fig. 7. Various reflection regimes, PBX 9501 onto uranium. Upper bar shows region (M) of theoretically possible Mach reflection with positive rate of growth of Mach stem. Lower bar shows range of regular shock reflection (R) solutions and also the range (R-PM) of reflected Prandtl-Meyer rarefactions.
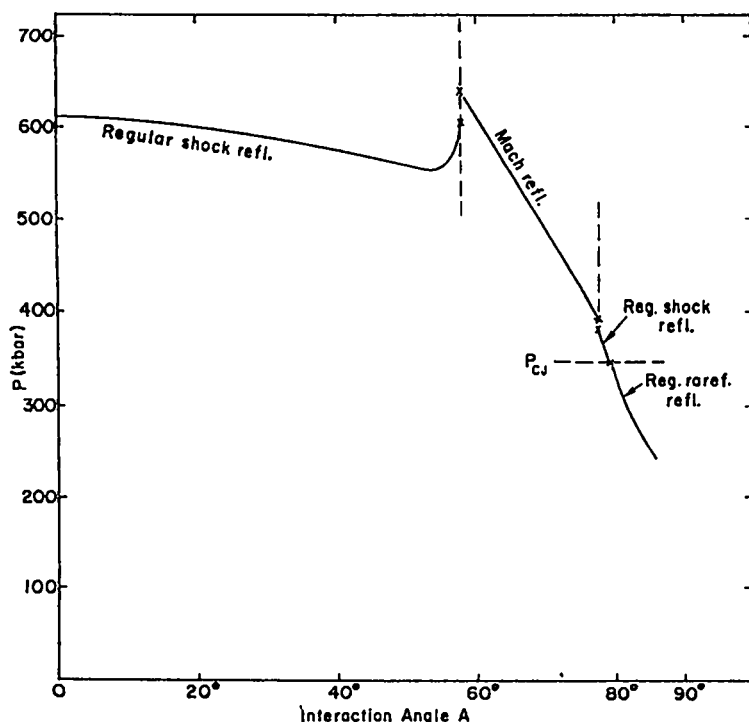
Fig. 8. Metal-shock pressure vs interaction angle for a PBX 9501 detonation wave onto uranium.

reflected shock into the explosive has zero strength and the metal-shock pressure equals the explosive Chapman-Jouguet pressure) and A = 90°, the wave that is reflected into the explosive is a rarefaction (a Prandtl-Meyer wave).

VI. CONCLUDING REMARKS AND FURTHER WORK

In addition to assuming a straight stem in the Mach regime, we have (a) selected the weak root for regular reflection and (b) selected regular reflection in the range where both types are theoretically possible. These apparently reasonable assumptions are in fact unproved, and it is of interest to look briefly at some of the consequences of error in either or both. If (b) is wrong and (a) is right, the transition from regular to Mach reflection will occur at A = 57.38°, some 0.7° sooner. This would cause the associated jump in pressure to be around 75 kbar instead of the 30 kbar reported. Next, if (a) is wrong [and regardless of (b)], there would apparently have to be a very large discontinuity in P somewhere within the regular reflection regime beween A = 0° (where the weak root agrees with the value for head-on reflection) and A = 58.1°. It is only in the very unlikely event that (a) and (b) are both wrong that one would avoid the discontinuity in P at the regular-to-Mach transition. Then it can be shown that the strong root for regular reflection agrees in pressure with the Mach solution.

12

This would hardly simplify life, however, because one would still be stuck with the discontinuity in P somewhere within the regular reflection regime. As already mentioned, our best guess is that (a) and (b) are both true and that Fig. 8 is a reasonable best estimate of metal-shock pressure vs angle A for PBX 9501 onto uranium.

APPENDIX
EXTENSION TO OTHER METALS

Calculations have also been performed for PBX 9501 onto tantalum, copper, 304 stainless steel, aluminum, and nickel using the metal equation-of-state constants listed in Ref. 4.

The resulting curves for metal-shock pressure vs angle A are seen as Fig. A-1. Tantalum, steel, and nickel are qualitatively similar to uranium in their interactions with PBX 9501.

(1) A regular reflection regime extends from $A = 0°$ to $A = 62° \pm 4°$. Metal-shock pressure rises steeply near the end of this regime, and the transition to Mach reflection is marked by a discontinuous jump in pressure.
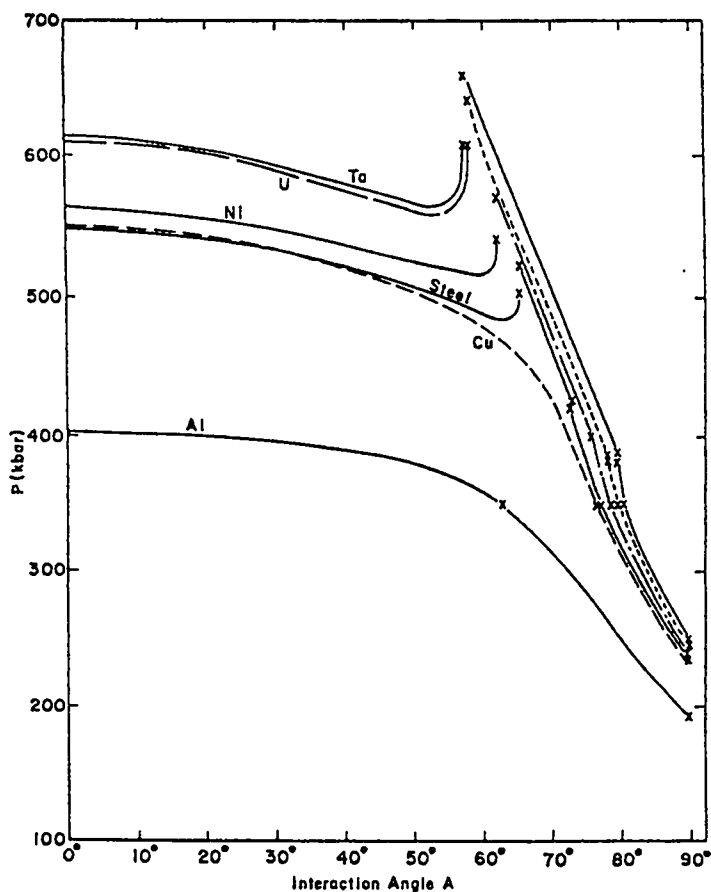
Fig. A-1. Shock pressure for six metals vs angle of incidence A of a PBX 9501 detonation wave.

14

(2) A Mach reflection regime that is some 7° wide in steel increases to about 22° in tantalum. The metal-shock pressure drops off rapidly with increasing A in the Mach regime.

(3) A high-angle regular shock reflection regime, about 5° wide in steel, decreases to about 1° in tantalum. The transition from Mach reflection to this high-angle regular reflection is characterized by another (smaller) discontinuity in metal-shock pressure. As before, the Mach shock is stronger (again, because it utilizes the strong root for the reflected shock in the explosive).

(4) A reflected rarefaction regime at grazing incidence begins as early as 77° for steel and as late as 80° for tantalum. This regime continues to A = 90°, the largest angle considered. Within this rarefaction regime, the pressure decreases from the explosive Chapman-Jouguet pressure (348.8 kbar) to 240 ± 10 kbar for the four metals being considered.

Copper and aluminum are qualitatively different from the other four metals (in their interactions with PBX 9501), in that they do not cause Mach reflection within the explosive. Regular shock reflection occurs up to the onset of the reflected rarefaction regime, and there are no discontinuities in the curve of metal-shock pressure vs incidence angle A.

Table A-I repeats some representative points on the P vs A curves, and Table A-II gives critical angles and associated pressures.

For several metals, T. R. Neal[5] measured the shock pressures caused by a PBX 9404 detonation wave at grazing (A = 90°) incidence. Three of his metals are ones calculated here, so comparisons can be made if one neglects the apparently small differences between PBX 9404 and PBX 9501. He measured 248 ± 12 kbar for uranium, 235 ± 11 kbar for copper, and 199 ± 1 kbar for aluminum. The present calculated values of 239, 227, and 189 kbar are low by 3.6%, 3.4%, and 5.0%, respectively. The first two values are within Neal's standard deviations, but our value for aluminum is significantly low. Additional experiments are now in progress (PBX 9501 onto uranium) to check the calculations at intermediate angles.

In continuing computational work, we will be concerned with the metal heating caused by these shock waves and with correlating the heating from this and other sources with the observed performance of these metals in jet-generator devices.

TABLE A-I

METAL-SHOCK PRESSURES kbar FOR VARIOUS ANGLES OF INCIDENCE
OF A PBX 9501 DETONATION WAVE

	0°	10°	20°	30°	40°	50°	60°	70°	80°	89.5°
U	609.9	608.1	600.7	589.0	574.4	561.0	607	487	339.9	244.2
Ta	614.3	611.2	604.3	593.4	580.2	569.7	609	493	348.8	250.8
Cu	551.1	548.7	543.1	533.7	520.5	503.1	479.5	424.5	309.4	230.8
304 SS	549.0	546.6	541.7	533.6	522.1	507.2	489.1	458	315.9	233.8
Al	401.9	401.2	399.4	396.0	390.1	379.2	357.7	314.0	249.4	192.1
Ni	564.1	562.7	557.6	549.1	537.7	524.3	516.6	472	327.3	239.6

TABLE A-II

VALUES OF VARIABLES AT CRITICAL POINTS

	A_1	P_1(kbar)	A_2	P_2(kbar)	A_3	P_3(kbar)
U	58.07	609.1/640	77.81	382.9/386	79.38°	348.8
Ta	57.30	609.2/659	79.30	371.1/378	80.37°	348.8
Cu	------	---------	------	---------	76.28°	348.8
304 SS	65.26	501.8/522	72.40	420.7/425	77.05°	348.8
Al	------	---------	------	---------	62.66°	348.8
Ni	61.96	540.6/572	75.65	395.4/401	78.26°	348.8

REFERENCES

1. H. M. Sternberg and D. Piacesi, "Interaction of Oblique Detonation Waves with Iron," Phys. Fluids 9, No. 7, 1307-1351 (July 1966).

2. S. D. Gardner and J. D. Wackerle, "Interactions of Detonation Waves in Condensed Explosives," Preprint, Proc. Symp. Detonation, 4th, White Oak, Maryland, October 12-15, 1965 (Office of Naval Research, Washington, DC, 1966), pp. A129-A140. See also abstract (Office of Naval Research, Washington, DC, 1965) ACR-126, pp. 155-156.

3. A. K. Oppenheim, J. J. Smolen, D. Kwak, and P. A. Urtiew, "On The Dynamics of Shock Intersections," Proc. Symp. Detonation, 5th, Pasadena, California, August 18-21, 1970 (Office of Naval Research, Washington, DC, 1970), ACR-184, pp. 119-138.

4. J. M. Walsh, "Dimensionless Equation of State for Condensed Media - Numerical Results for Shock Heating and for Flow Deflection by an Oblique Stationary Shock," Los Alamos National Laboratory report LA-9516-MS (September 1982).

5. T. R. Neal, "Perpendicular Explosive Drive and Oblique Shocks," Proc. Symp. Detonation, 6th, Naval Service Weapons Center, Coronado, California, August 24-27, 1976 (Office of Naval Research, Washington, DC, 1976), ACR-221, pp. 602-611.
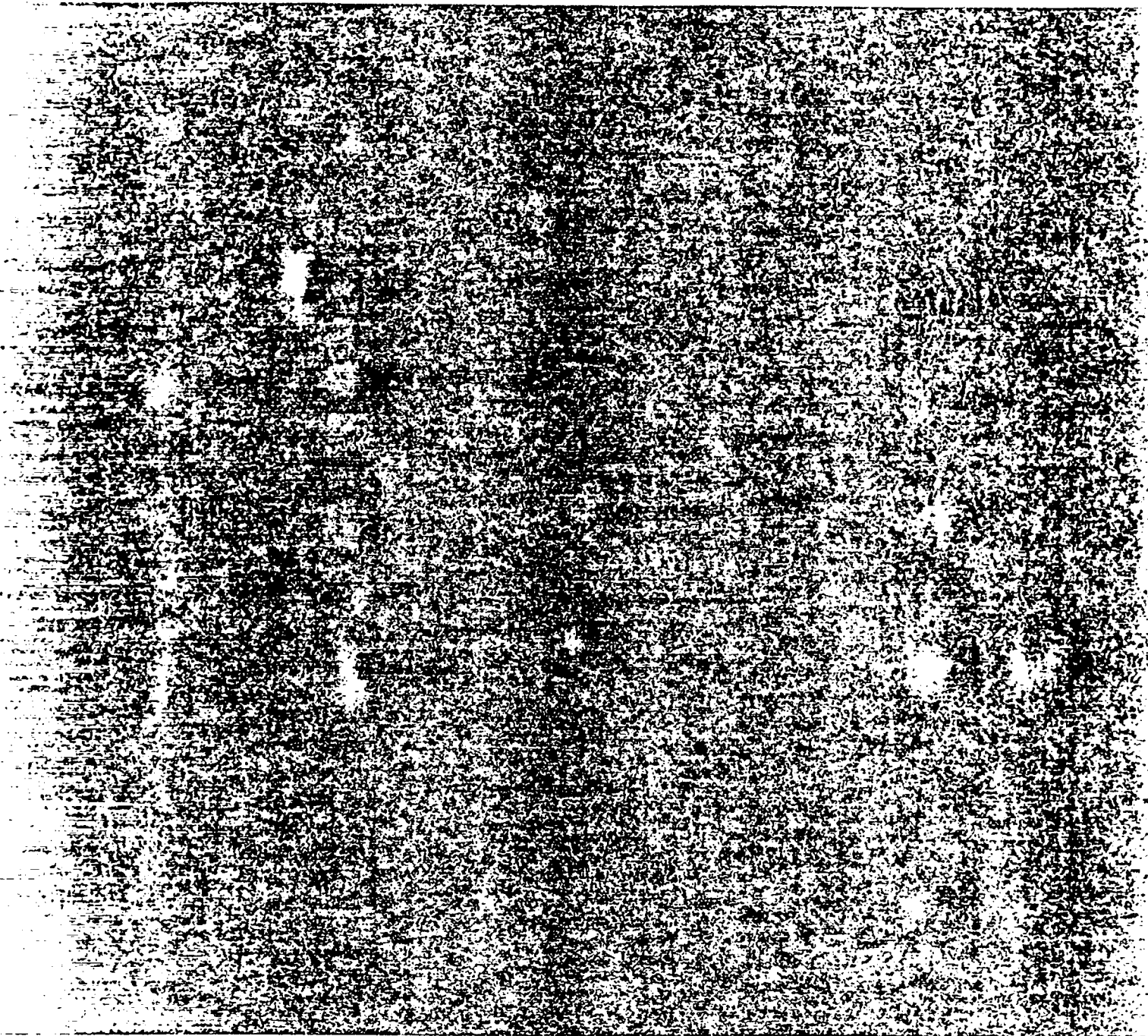
Page Range	NTIS Price Code	Page Range	NTIS Price Code	Page Range	NTIS Price Code	Page Range	NTIS Price Code
001-025	A02	151-175	A08	301-325	A14	451-475	A20
026-050	A03	176-200	A09	326-350	A15	476-500	A21
051-075	A04	201-225	A10	351-375	A16	501-525	A22
076-100	A05	226-250	A11	376-400	A17	526-550	A23
101-125	A06	251-275	A12	401-425	A18	551-575	A24
126-150	A07	276-300	A13	426-450	A19	576-600	A25
						601-up*	A99

*Contact NTIS for a price quote.

Los Alamos